

Foreshocks and Earthquake Predictability

A. Helmstetter¹ and D. Sornette^{1 3}

¹ Institute of Geophysics and Planetary Physics
University of California, Los Angeles, California 90095

² Department of Earth and Space Science
University of California, Los Angeles, California 90095

³ Laboratoire de Physique de la Matière Condensée
CNRS UMR6622 and Université des Sciences, Parc Valrose, 06108 Nice Cedex 2, France

Abstract: The observation of foreshocks preceding large earthquakes and the suggestion that foreshocks have specific properties that may be used to distinguish them from other earthquakes have raised the hope that large earthquakes may be predictable. Among proposed anomalous properties are the larger proportion than normal of large versus small foreshocks, the power law acceleration of seismicity rate as a function of time to the mainshock and their spatial migration toward the mainshock, when averaging over many sequences. Using Southern California seismicity, we show that these properties and others arise naturally from the simple model that any earthquake may trigger other earthquakes. This model puts all earthquakes on the same footing. We find that foreshocks precursory properties are independent of the mainshock size. This implies that earthquakes (large or small) are predictable to the same degree as seismicity rate is predictable from past seismicity by taking into account cascades of triggering.

1 Foreshocks, mainshocks and aftershocks: hypothesis and predictions

It has been recognized for a long time that large earthquakes are sometimes preceded by an acceleration of the seismic activity, known as foreshocks [1, 2]. In addition to the increase of the seismicity rate a few hours to months before large earthquakes, other properties of foreshocks have been reported, which suggest their usefulness (when present) as precursory patterns for earthquake prediction. Because foreshocks are rare and it is believed that a good proportion of them are forerunners of large events, specific physical mechanisms have been proposed for them with the hope of helping earthquake prediction [3]-[6]. In addition, anomalous precursory seismic activity extending years to decades before large earthquakes and at distances up to ten times the mainshock rupture size are often thought to require different physical mechanisms [7]-[12] than for foreshocks closer to the mainshock epicenters.

The division between foreshocks, mainshocks, and aftershocks has a long and distinguished history in seismology. Within a pre-specified space-time domain, foreshocks are usually defined as earthquakes (above the background rate) preceding a larger earthquake (mainshock), which is itself followed by an increase in seismicity of smaller earthquakes (aftershocks). However, recent empirical and theoretical scrutiny suggests that this division might be arbitrary and physically artificial [13]-[17]. Since the underlying physical processes are not fully understood, the qualifying time and space windows used to select aftershocks, mainshocks and aftershocks are more based on common sense than on hard science. If the space-time window is extended and a new event not considered previously is found with a magnitude larger than the previously classified mainshock, it becomes the new mainshock and all preceding events are retrospectively called foreshocks. A clear identification of foreshocks, aftershocks and mainshocks is hindered by the fact that nothing distinguishes them in their seismic signatures: at the present level of resolution of seismic inversions, they are found to have the same double-couple structure and the same radiation patterns [14]. Statistically, the aftershock magnitudes are distributed according to the Gutenberg-Richter (GR) distribution $P(m) \sim 10^{-bm}$ with a similar b -value to other earthquakes [18, 19]. However, some studies [19, 20, 21] have suggested that foreshocks have a smaller b -value than other earthquakes, but the physical mechanisms are not yet understood. Moreover, an event can be both an aftershock of a preceding large event, and a mainshock of a following earthquake. For example, the $M=6.5$ Big Bear event is usually considered as an aftershock of the $M=7.3$ Landers event, and has clearly triggered its own aftershock sequence.

The Omori law describes the power law decay of the aftershock rate $\dot{N} = (t - t_c)^{-p}$ with time from a mainshock that occurred at t_c [22]-[24], and which may last from months up to decades. In contrast with the well-defined Omori law for aftershocks, there are huge fluctuations of the foreshock seismicity rate, if any, from one sequence of earthquakes to another one preceding a mainshock, as shown in figure 1. By stacking many foreshock sequences, a well-defined acceleration of the seismicity preceding mainshocks emerges,

quantified by the so-called inverse Omori law $\lambda = (\tau_c - t)^{p^0}$, where τ_c is the time of the mainshock [25, 23, 26]. The inverse Omori law is usually observed for time scales shorter than the direct Omori law, of the order up to weeks to a few months before the mainshock. However, there seems to be no way of identifying foreshocks from usual aftershocks and mainshocks in real time (see [15, 14] for a pioneering presentation of this view point). In other words, is the division between foreshocks, mainshocks and aftershocks falsifiable [27]?

In order to address this question, we present a novel analysis of seismic catalogs, based on a parsimonious model of the classification of foreshocks, mainshocks and aftershocks, in terms of earthquake triggering: earthquakes may trigger other earthquakes through a variety of physical mechanisms [28] but this does not allow one to put a tag on them. Thus, rather than keeping the specific classification that foreshocks are precursors of mainshocks and mainshocks trigger aftershocks, we start from the following hypothesis:

Hypothesis 1 *Using the essential idea of triggered seismicity in time and space, a parsimonious description of seismicity does not require the division between foreshocks, mainshocks and aftershocks that are indistinguishable from the point of view of their physical processes.*

The simplest construction that embodies the Hypothesis is the epidemic-type aftershock (ETAS) model introduced in [16, 29] (in a slightly different form) and in [30], which is described in the technical part 7. In this model, all earthquakes may be simultaneously mainshocks, aftershocks and possibly foreshocks. An observed “aftershock” sequence in the ETAS model is the sum of a cascade of events in which each event can trigger more events. The triggering process may be caused by various mechanisms that either compete or combine, such as pore-pressure changes due to pore-fluid flows coupled with stress variations, slow redistribution of stress by aseismic creep, rate-and-state dependent friction within faults, coupling between the viscoelastic lower crust and the brittle upper crust, stress-assisted micro-crack corrosion, etc.. The ETAS model has been used previously to give short-term probabilistic forecast of seismic activity [29, 31, 32], and to describe the temporal and spatial clustering of seismic activity [30]-[33, 17]. The Hypothesis and the ETAS model allow us to study two classes of foreshocks, called of type I (associated with conditioned mainshocks) and of type II (associated with unconditioned mainshocks), defined in the technical part 6.

The simple embodiment of the Hypothesis in the ETAS model leads to the following consequences and predictions [34], which are proposed as crucial tests of the Hypothesis.

1. The rate of foreshocks of type II is predicted to increase before the mainshock according to the inverse Omori law $\lambda = (\tau_c - t)^{p^0}$ with an exponent p^0 smaller than the exponent p of the direct Omori law. The exponent p^0 depends on the “local” Omori exponent $1 + \beta$ describing the direct triggering rate between earthquakes (first-generation triggering), on the b -value of the GR distribution and on the exponent α quantifying the increase $\sim 10^{\alpha M}$ in the number of aftershocks as a function of the magnitude M of the mainshock [39]. The inverse Omori law also holds for foreshocks of type I preceding large mainshocks.

2. In contrast with the direct Omori law, which is clearly observed after all large earthquakes, the inverse Omori law is a statistical law, which is observed only when stacking many foreshock sequences. In this way, it may be possible to detect foreshocks years and up to decades before the mainshock and at distance of up to two hundred kilometers from the mainshock (see figures 3 and 4 below).
3. While the number of aftershocks increases as 10^M with the magnitude M of the mainshock, the number of foreshocks of type II is predicted to be independent of M . Thus, the seismicity should increase on average according to the inverse Omori law before any earthquake, whatever its magnitude. For foreshocks of type I, the same results should hold for large mainshocks. For small and intermediate values of the mainshock magnitude M , the conditioning on foreshocks of type I to be smaller than their mainshock makes their number increase with M solely due to the constraining effect of their definition.
4. The GR distribution for foreshocks is predicted to change upon the approach of the mainshock, by developing a bump in its tail. Specifically, the modification of the GR law is predicted to take the shape of an additive correction to the standard power law, in which the new term is another power law with exponent b . The amplitude of this additive power law term is predicted to also exhibit a power law acceleration upon the approach to the mainshock.
5. The spatial distribution of foreshocks is predicted to migrate toward the mainshock as the time increases toward the time of the mainshock, by the mechanism of a cascade of seismic triggering leading to a succession of jumps like in a continuous-time random walk [41].

We now proceed to test systematically these predictions on the catalog of the Southern California Data Center (SCEC) over the period 1932-2000, which is almost complete above $M = 3$ and contains more than 22000 $M \geq 3$ earthquakes, using the methodology described in the technical part 6.

2 Direct and inverse Omori law

Figure 2 shows the rate of foreshocks of type II as a function of $t_c - t$ and of aftershocks as a function of $t - t_c$, where t_c is the time of the mainshocks, with the space-time window ($T = 1$ yr; $R = 50$ km). Both rates follow an approximate power law (inverse Omori law for foreshocks with exponent p^0 and Omori law for aftershocks with exponent p). The fluctuations of the data makes it hard to exclude the hypothesis that the two power laws have the same exponent $p = p^0 = 1$; even if p^0 seems slightly smaller. Note that it can be shown theoretically for $b < b=2$ that $p = 1$ and $p^0 = 1 - 2$ for a local Omori law with exponent $1 +$ and that the difference $p - p^0$ should get smaller as b increases above $b=2$ [34]. Since $b = 0.8 > b=2 = 0.5$, this limit is met which explains the smallness of the difference $p - p^0$.

The second striking observation is the strong variation of the amplitude of the rate $N_a(t)$ of aftershocks as a function of the magnitude M of the mainshock, which is well-captured by an exponential dependence $N_a(t) / 10^M = (t - t_c)^p$ with $p = 0.8$ [39]. In contrast, the rates of foreshocks of type II are completely independent of the magnitude M of the mainshocks: quite strikingly, all mainshocks *independently* of their magnitudes are preceded by the same statistical inverse Omori law, with the same power law increase and the same absolute amplitude! All these results are very well modeled by the ETAS model with the parameters $\alpha = 0.8$, $\beta = 0.2$ and $b = 1$ using the theoretical framework and numerical simulations developed in Ref. [34].

Another remarkable observation is presented in figure 3 which shows the rate of foreshocks of type II for mainshock magnitudes between 4 and 4.5, for different values of the distance R used to select aftershocks and foreshocks. The inverse Omori law is observed up to $R = 200$ km, and the duration of the foreshock sequences increases as R decreases due to the decrease of the effect of the background seismicity. Restricting to the shortest distances R to minimize the impact of background seismicity, the inverse Omori laws can be observed up to 10 yrs before mainshocks, for foreshocks of type II (figure 4). Thus, foreshocks are not immediate precursors of mainshocks but betray an organizing process acting over very long time and large distances. However, this organizing process operates entirely through the cascade of triggering embodied in the familiar Omori law.

An important question concerns the relative weight of coincidental shocks, i.e., early aftershocks triggered by a previous large earthquake, which appear as foreshocks of type II to subsequent aftershocks. Such coincidental shocks can give rise to an apparent inverse Omori law [13] when averaging over all possible positions of “mainshocks” in the sequence, without any direct interaction between these mainshocks and preceding events viewed as their foreshocks. Actually, these coincidental shocks form a minority of the total set, because the fraction of shocks directly triggered by a mainshock decays to negligible values beyond a few days for the range of parameters of the ETAS that realistically fit the SCEC catalog [17, 34].

Figure 5 shows the rate of foreshocks of type I as a function of $t_c - t$ and of aftershocks as a function of $t - t_c$, where t_c is the time of the mainshocks. There are much larger fluctuations for foreshocks of type I than for foreshocks of type II due to the smaller number of the former. Nevertheless, an increase of the seismicity before a mainshock for foreshocks of type I is clearly visible, which implies that large mainshocks can be triggered by smaller earthquakes. The exponent p^0 of the inverse Omori law for foreshocks of type I is approximately equal to the exponent of foreshocks of type II and to the exponent p of the direct Omori law for aftershocks. The rate of foreshocks of type I increases slowly with the mainshock magnitude but this increase is not due to a larger predictability of larger earthquakes, as expected for example in the critical point theory [11] and as observed in a numerical model of seismicity [38]. The increase of the number of type I foreshocks with the mainshock magnitude can be reproduced faithfully in synthetic catalogs generated with the ETAS model and is nothing but the consequence of the algorithmic rules used to define foreshocks of type I: the smaller the mainshock magnitude, the more drastic is the selection and the pruning of foreshocks [34]. In other words, there is no physics but only statistics

in the weak increase of foreshocks of type I with the mainshock magnitude. Confirming this concept, the inverse Omori law for foreshocks of type I becomes independent of the mainshock magnitudes M for large M , for which the selection constraint has only a weak statistical effect. The dependence of the inverse Omori law for foreshocks of type I as a function of distance R used to select foreshocks is very similar (not shown) to that shown for foreshocks of type II in figure 3, but the duration of foreshock sequences is shorter for type I foreshocks.

3 Modification of the magnitude distribution before a mainshock

Let us state precisely the predictions of the ETAS model based only on the concept of triggering between earthquakes. We refer to [34] for the derivation of the results stated below, which is too involved to be reported here. Intuitively, the essence of the mathematical derivation in Ref. [34] is that the inverse Omori law emerges as the expected (in a statistical sense) trajectory of seismicity, conditioned on the fact that it leads to the burst of seismic activity accompanying the mainshock (independently of its magnitude). This conditioned seismic activity leads itself to a conditional Gutenberg-Richter distribution which is different from the normal or unconditional Gutenberg-Richter distribution. Thus, conditioning a seismic sequence to end at a mainshock, the distribution $P(m)$ of foreshock magnitudes is predicted to get an additive (or deviatoric) power law contribution $q(t)dP(m)$ with an exponent smaller than b and with an amplitude $q(t)$ growing as a power law of the time to the mainshock:

$$P(m) = (1 - q(t))P_0(m) + q(t) dP(m); \quad (1)$$

where $P_0(m)$ is the standard GR distribution $P_0(m) = 10^{-bm}$ and $dP(m) = 10^{-b^0 m}$ with $b^0 = b - \epsilon$. The amplitude $q(t)$ of the deviatoric distribution in (1) should increase as a power-law of the time to the mainshock according to

$$q(t) = 1 - (t_c - t)^{-\frac{b^0}{\epsilon}}; \quad (2)$$

This analytical prediction has been checked with extensive numerical simulations of the ETAS model. Intuitively, the additional deviatoric distribution $dP(m)$ results from the increase of the number of triggered events with the mainshock magnitude. The magnitude distribution of triggering events is given by the product $(m)P_0(m) = 10^{-m} 10^{-bm} dP(m)$, which gives the distribution of foreshock magnitudes for large m .

We now test this prediction using the SCEC catalog on foreshocks of type II of $M > 3$ mainshocks, selected using $R = 20$ km and $T = 1$ yr. The magnitude distribution $P(m)$ sampled at different times before mainshocks is shown in panel (a) of figure 6, where the blue to red curves correspond to times preceding mainshocks decreasing from 1 year to 0.01 day with a logarithmic binning. As time approaches that of the mainshocks, one can clearly observe that the tails depart more and more from the standard GR power law $P_0(m)$ with $b = 0.95 \pm 0.1$ estimated using the whole catalog and shown as the dashed line.

The deviatoric part $q(t)dP(m)$ in (1) of the foreshock magnitude distribution, shown in panel c) of figure 6, can be estimated by fitting the prediction (1) to the observed magnitude distribution of foreshocks, by inverting the parameters b^0 and $q(t)$ in (1) for different times before mainshocks. The obtained deviatoric GR laws $q(t)dP(m)$ are compatible with pure power laws with an approximately constant exponent $b^0 = 0.6 \pm 0.1$ shown in panel (d) of figure 6. The amplitude $q(t)$ is shown in panel (b) and is compatible with a power law (2) with a fitted exponent 0.3 ± 0.2 . These observations are in good qualitative agreement with the predictions (1) and (2) on the nature of the modification of the GR law for foreshocks in terms of a pure deviatoric power law component with an amplitude growing as a power law of the time to the mainshocks.

Note that expression (1) contains as a special case the model in which the modification of the GR law occurs solely by a progressive decrease of the b -value as the time of the mainshock is approached (by putting $q(t) = 1$ and allowing b^0 to adjust itself as a function of time), as proposed in [23, 40, 20, 21]. Our quantitative analysis clearly excludes this possibility while being completely consistent with the mechanism embodied by the concept of triggered seismicity that mainshocks are conditional aftershocks of foreshocks [34]. Although the foreshock magnitude distribution is not a pure power-law but rather the sum of two power laws, our results rationalize the reported decrease of b -value before mainshocks [23, 40, 20, 21]. Indeed, with a limited number of events, the sum of two power laws predicted by (1) with an increasing weight of the deviatoric part as the time of the mainshock is approached will be seen as a decreasing b -value when fitted with a single GR power law.

4 Migration of foreshocks

The last prediction discussed here resulting from the Hypothesis is that foreshocks should migrate slowly toward the mainshock. Note that the specification (4) of the ETAS model in the technical part 7 predicts no diffusion or migration if seismicity results solely from direct triggering (first generation from mother to daughter). Technically, this results from the separability of the space and time dependence of $M_i(t, \mathbf{x}_i, \mathbf{x}_i)$. In the ETAS model, diffusion and migration can be shown to result from the cascade of secondary, tertiary (and so on) triggered seismicity, akin to a (continuous-time) random walk with multiple steps [41], which couples the space and time dependence of the resulting global seismicity rate. Assuming a cylindrical symmetry valid at large distances from the mainshocks, this migration or anti-diffusion of the seismic activity toward the mainshock is quantified by the characteristic size R of the cluster of foreshocks which is predicted to decrease before the mainshock according to [34, 41]

$$R = (t_c - t)^H ; \quad (3)$$

with $H = \frac{1}{2} + \frac{1}{2} \frac{1}{\beta}$ for $\beta < 2$ where β and γ are defined in the technical insert 7. It is natural that the (sub-)diffusive exponent H combines the exponent β (respectively γ) of the time- (resp. space-) dependent local processes (6) and (7). This law (3) describes the localization

of the seismicity as the mainshock approaches, which is also observed in real seismicity [23, 42].

We use a superposed epoch analysis and stack all sequences of foreshocks of type II synchronized at the time of the mainshock and with a common origin of space at the location of each mainshock. The analysis of the California seismicity presented in inset of Figure 4 shows clearly a migration of the seismicity toward the mainshock, confirmed by the significant diffusion exponent $H = 0.3 \pm 0.1$. This value is compatible with the estimates $\alpha = 0.2$ and $\beta = 1$. However, this migration is likely to be an artifact of the background activity, which dominates the catalog at long times and distances from the mainshocks. Indeed, the shift in time from the dominance of the background activity at large times before the mainshock to that of the foreshock activity clustered around the mainshock at times just before it may be taken as an apparent inverse diffusion of the seismicity rate when using standard quantifiers of diffusion processes (see [41] for a discussion of a similar effect for the apparent diffusion of aftershocks).

5 Conclusions

By defining the foreshocks of type II and by comparing them with standard foreshocks of type I, we have followed Freeman Dyson who wrote that, “the effect of a concept-driven revolution is to explain old things in new ways.” [43]. We have thus revisited the phenomenology of earthquake foreshocks using the point of view of triggered seismicity formulated in our Hypothesis. We have found that the most salient properties of foreshock sequences are explained solely by the mechanism of earthquake triggering. This validates the Hypothesis.

An important result is that the precursory modification of the seismic activity before a mainshock is independent of its magnitude, as expected by the triggering model with a constant magnitude distribution. Therefore, large earthquakes are not better predictable than smaller earthquakes on the basis of the power-law acceleration of the seismicity before a mainshock or by using the modification of the magnitude distribution. The increase of the number of standard foreshocks of type I with the mainshock magnitude is found to result solely from the sorting algorithm and does not reflect any deep physical mechanism.

All these results taken together stress the importance of the multiple cascades of earthquake triggering in order to make sense of the complex spatio-temporal seismicity. In particular, our results do not use any of the specific physical mechanisms proposed earlier to account for some of the observations analyzed here. For instance, the ETAS model is different from the receding stress shadow model [44, 11] and from the critical earthquake model [9, 10, 11] which in addition each addresses only a specific part of the seismic phenomenology. Our demonstration and/or confirmations of (i) the increase of rate of foreshocks before mainshocks (ii) at large distances and (iii) up to decades before mainshocks, (iv) a change of the Gutenberg-Richter law from a concave to a convex shape for foreshocks, and (v) the migration of foreshocks toward mainshocks are reminiscent of, if not identical to, the precursory patterns documented in particular by the Russian [7, 12]

and Japanese [45] schools, whose physical origin has remained elusive an/or controversial. The present work suggests that triggered seismicity is sufficient to explain them.

Acknowledgments: We are grateful to E. Brodsky, J.-R. Grasso, H. Houston, Y.Y. Kagan, G. Ouillon and J. Vidale for stimulating discussions and a critical reading of the manuscript. This work was partially supported by the James S. Mc Donnell Foundation 21st century scientist award/studying complex system.

6 First technical part: Definition of foreshocks of type I and of type II

6.1 Formal definitions

The usual definition of foreshocks, that we shall call “foreshock of type I,” refers to any event of magnitude smaller than or equal to the magnitude of the following event, then identified as a “mainshock.” This definition implies the choice of a space-time window (R, T) used to define both foreshocks and mainshocks. Mainshocks are large earthquakes that were not preceded by a larger event in this space-time window. The same window can be used to select foreshocks before mainshocks in a systematic search procedure. All previous studies published in the literature dealt with foreshocks of type I.

In contrast, the Hypothesis makes it natural to define “foreshock of type II,” as any earthquake preceding a large earthquake which is defined as the mainshock, independently of the relative magnitude of the foreshock compared to that of the mainshock. This second definition will thus incorporate seismic sequences in which a foreshock could have a magnitude larger than the mainshock, a situation which can alternatively be interpreted as a mainshock followed by a large aftershock. The advantage of this second definition is that foreshocks of type II are automatically defined as soon as one has identified the mainshocks, for instance, by calling mainshocks all events of magnitudes larger than some threshold of interest. Foreshocks of type II are thus all events preceding these large magnitude mainshocks. In contrast, foreshocks of type I need to obey a constraint on their magnitude, which may be artificial, as we shall see further down.

6.2 Practical implementation

In our analysis of the SCEC catalog, we construct foreshock and aftershock sequences as follows. A mainshock is defined as an earthquake in the magnitude range $(M; M + M)$ that was not preceded by a larger event in a space-time window (R_2, T) before the mainshock. The distance $R_2 = 50$ km is here chosen to be close to (but smaller than) the maximum size of the spatial clusters of seismicity in the California catalog, in order to minimize the influence of large earthquakes that occurred before the mainshock. Other choices between 20 km to 200 km have been tested and give essentially the same results. The aftershocks are all events that occurred in a space-time window (R, T) after each mainshock. The foreshocks of type I are selected in a space-time window (R, T) before each mainshock.

Since our purpose is to test the Hypothesis, which avoids the usual preconception on foreshocks/mainshocks/aftershocks, we also consider foreshocks of type II defined as the events in a space-time window (R, T) before each mainshock, now defined without the constraint that they were not preceded by a larger event in a space-time window (R_2, T) . The difference between foreshocks of type I and of type II is that the selection of their respective mainshocks is different, the mainshocks of the former being rather arbitrary and the corresponding foreshocks being very sensitive to the choice of the space-window $(R_2,$

T) used to select their mainshocks.

We use a superposed epoch analysis to stack all foreshocks and aftershocks sequences synchronized at the time of the “mainshocks” in different mainshock magnitude intervals, and for different choices of the space-time window R, T used to define foreshocks and aftershocks. R has been tested between 10 km and up to 500 km with no essential change, except for an increasing sensitivity to the background seismicity for the largest R (see figure 3). T has been tested between 0.5 year to 10 years with similar results. Tests have also been performed with the spatial window size R adjusted to scale with the mainshock magnitude with no significant difference. Our results presented below thus appear very robust with respect to the (arbitrary) definitions of the space-time windows and the definition of mainshocks. In the main text, foreshocks of type I and of type II are treated separately. We use larger magnitude intervals ΔM for larger mainshock magnitudes to compensate for the smaller earthquake populations. Previous studies of foreshocks using superposed epoch analysis [35, 36, 1, 26, 23, 13, 37] have considered foreshocks of type I only.

7 Second technical part: Definitions of the ETAS model

The epidemic-type aftershock (ETAS) model assumes that a given event (the “mother”) of magnitude m_i occurring at time t_i and position \mathbf{x}_i gives birth to other events (“daughters”) of any possible magnitude m at a later time between t and $t + dt$ and at point $\mathbf{x} = \mathbf{x}_i + \mathbf{d}\mathbf{x}$ at the rate

$$\dot{m}_i(t, t_i; \mathbf{x}, \mathbf{x}_i) = \dot{m}_i(t, t_i) \dot{\mathbf{x}}(\mathbf{x}, \mathbf{x}_i) : \quad (4)$$

We will refer to $\dot{m}_i(t, t_i; \mathbf{x}, \mathbf{x}_i)$ as the “local” Omori law, giving the seismic rate induced by a single mother. It is the product of three independent contributions:

1. \dot{m}_i gives the number of daughters born from a mother with magnitude m_i . This term is in general chosen to account for the fact that large earthquakes have many more triggered events than small earthquakes. Specifically,

$$\dot{m}_i = K 10^{m_i} ; \quad (5)$$

which is justified by the power law dependence of the volume of stress perturbation as a function of the earthquake rupture size.

2. $\dot{t}(t, t_i)$ is a normalized waiting time distribution giving the rate of daughters born at time $t - t_i$ after the mother

$$\dot{t}(t) = \frac{c}{(t + c)^{1+\alpha}} ; \quad (6)$$

3. $\dot{\mathbf{x}}(\mathbf{x}, \mathbf{x}_i)$ is a normalized spatial “jump” distribution from the mother to each of her daughter, quantifying the probability for a daughter to be triggered at a distance $|\mathbf{x} - \mathbf{x}_i|$ from the mother. Specifically, we take

$$\dot{\mathbf{x}}(\mathbf{x}) = \frac{1}{d \left(\frac{|\mathbf{x} - \mathbf{x}_i|}{d} + 1 \right)^{1+\beta}} ; \quad (7)$$

which has the form of an (isotropic) elastic Green function dependence describing the stress transfer in an elastic upper crust. The exponent β is left adjustable to account for heterogeneity and the possible complex modes of stress transfers [41].

The last ingredient of the ETAS model is that the magnitude m of each daughter is chosen independently from that of the mother and of all other daughters according to the Gutenberg-Richter distribution

$$P(m) = \frac{b}{\ln(10)} 10^{-b(m - m_0)} ; \quad (8)$$

with a b -value usually close to 1. m_0 is a lower bound magnitude below which no daughter is triggered.

References

- [1] Jones, L. M., and P. Molnar, *Nature* 262, 677 (1976).
- [2] Abercrombie, R. E., and J. Mori, *Nature*, 381, 303-307 (1996).
- [3] Yamashita, T. and L. Knopoff, *Geophys. Journal* 96, 389-399 (1989).
- [4] Sornette, D., C. Vanneste and L. Knopoff, *Phys. Rev. A* 45, 8351-8357 (1992).
- [5] Dodge, D. D., G. C. Beroza and W.L. Ellsworth, *J. Geophys. Res.*, 101, 22,371-22,392 (1996).
- [6] Dieterich, J. H. and B. Kilgore, *Proc. Nat. Acad. Sci USA*, 93, 3787-3794 (1996).
- [7] Keilis-Borok, V. I. and L. N. Malinovskaya, *J. Geophys. Res.*, 69, 3019-3024 (1964).
- [8] Knopoff, L., Levshina, T., Keilis-Borok, V.I. and Mattoni, C., *J. Geophys. Res.* 101, 5779-5796 (1996).
- [9] Bowman, D. D., G. Ouillon, C. G. Sammis, A. Sornette and D. Sornette, *J. Geophys. Res.* 103, 24359-24372 (1998).
- [10] Jaume, S.C. and Sykes, L.R., *Pure Appl. Geophys.* 155, 279-305 (1999).
- [11] Sammis, S.G. and D. Sornette, *Proc. Nat. Acad. Sci. USA* 99, 2501-2508 (2002).
- [12] Keilis-Borok, V., *Ann. Rev. Earth Plan. Sci.* 30, 1-33 (2002).
- [13] Shaw B.E., *Geophys. Res. Lett.* 20, 907-910 (1993).
- [14] Hough, S.E. and L.M. Jones, *EOS, Transactions, American Geophysical Union* 78, N45, 505-508 (1997).
- [15] Jones, L. M., R. Console, F. Di Luccio and M. Murru, *EOS (suppl.)* 76, F388 (1995).
- [16] Kagan, Y. Y. and L. Knopoff, *J. Geophys. Res.*, 86, 2853-2862 (1981).
- [17] Felzer, K.R., T.W. Becker, R.E. Abercrombie, G. Ekström and J.R. Rice, in press in *J. Geophys. Res.* (2002).
- [18] Ranalli, G., *Annali di Geofisica* 22, 359-39 (1969).
- [19] Knopoff, L., Y.Y. Kagan and R. Knopoff, *Bull. Seism. Soc. Am.* 72, 1663-1676 (1982).
- [20] Molchan, G. M. and O. Dmitrieva, *Phys. Earth. Plan. Inter.*, 61, 99-112 (1990).
- [21] Molchan, G. M., T.L. Konrod and A.K. Nekrasova, *Phys. Earth. Plan. Inter.*, 111, 229-240 (1999).

- [22] Omori, F., J. Coll. Sci. Imp. Univ. Tokyo 7, 111-120 (1894).
- [23] Kagan, Y. Y. and L. Knopoff, Geophys. J. R. Astr. Soc. 55, 67-86 (1978).
- [24] Utsu, T., Y. Ogata and S. Matsu'ura, J. Phys. Earth 43, 1-33 (1995).
- [25] Papazachos, B. C., Bull. Seis. Soc. Am. 63, 1973-1978 (1973).
- [26] Jones, L. M., and P. Molnar, J. Geophys. Res. 84, 3596-3608 (1979).
- [27] Kagan, Y.Y., Pure Appl. Geophys. 155, 233-258 (1999).
- [28] Harris, R.A., Earthquake stress triggers, stress shadows, and seismic hazard, in *International Handbook of Earthquake and Engineering Seismology*, edited by W. H. L. Lee et al., Chapter 73, 48 pages (Chapman and Hall, New-York) (2001).
- [29] Kagan, Y.Y. and L. Knopoff, Science 236, 1563-1467 (1987).
- [30] Ogata, Y., J. Am. Stat. Assoc. 83, 9-27 (1988).
- [31] Kagan, Y.Y. and Jackson, D.D., Geophys. J. Int. 143, 438-453 (2000).
- [32] Console, R. and M. Murru, J. Geophys. Res. 166, 8699-8711 (2001).
- [33] Kagan, Y.Y., Geophys. J. Int. 106, 135-148 (1991).
- [34] Helmstetter, A., D. Sornette and J.-R. Grasso, in press in J. Geophys. Res. (cond-mat/0205499) (2002).
- [35] Papazachos, B. C., Ann., Geofis., 28, 497-515 (1975).
- [36] Papazachos, B., Tectonophysics, 28, 213-216 (1975).
- [37] Reasenber, P. A., J. Geophys. Res. 104, 4755-4768 (1999).
- [38] Huang, Y., Saleur, H., Sammis, C. and Sornette, D., Europhys. Lett. 41, 43-48 (1998).
- [39] Helmstetter, A, submitted to *Geophys. Res. Letts.*, (cond-mat/0210056).
- [40] Berg, E., *Nature*, 219, 1141-1143, 1968.
- [41] Helmstetter, A. and D. Sornette, in press in *Phys. Rev. E.* (cond-mat/0203505).
- [42] von Seggern, D., S. S. Alexander and C-B Baag, *J. Geophys. Res.*, 86, 9325-9351, 1981.
- [43] Dyson, F., *Imagined worlds* (Cambridge, Mass.: Harvard University Press, 1997),
- [44] Bowman, D.D. and King, G.C.P., Geophys. Res. Lett. 28, 4039-4042 (2001).
- [45] Mogi, K., J. Phys. Earth 43, 533-561 (1995).

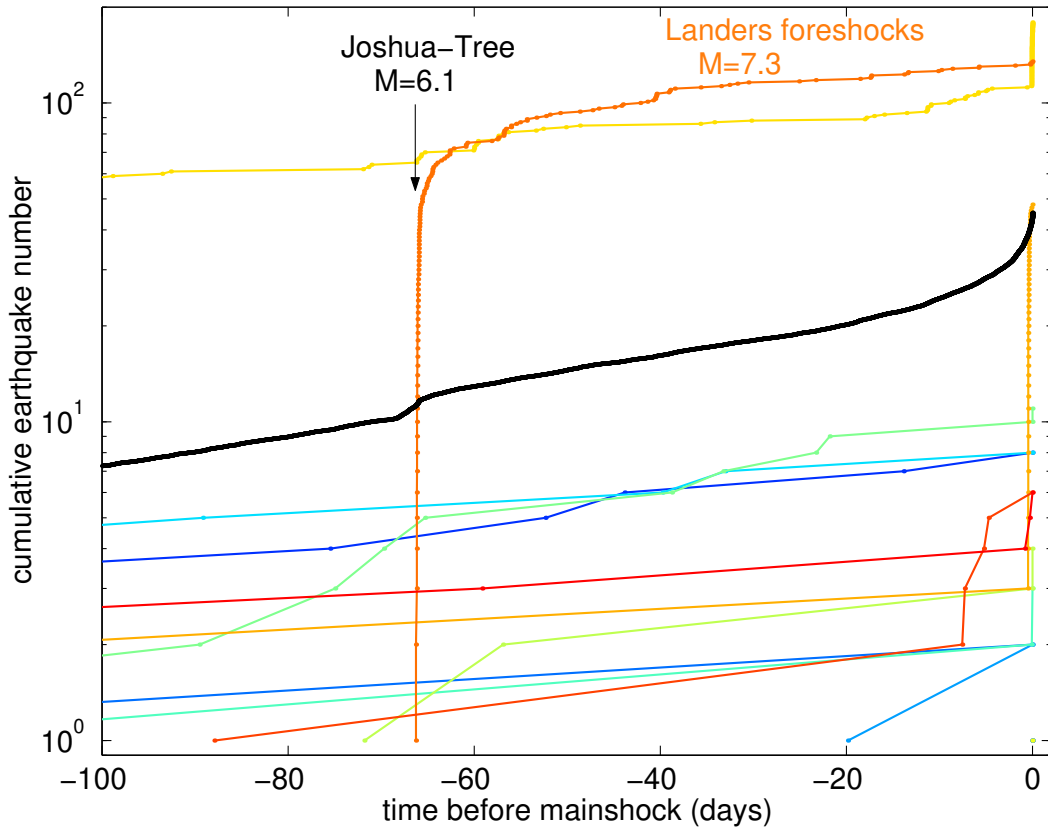


Figure 1: Cumulative number of foreshocks of type II (see definition in technical part 6) for all $M \geq 6.5$ mainshocks (thin color lines), and average number of foreshocks per mainshock (heavy black line), obtained by stacking all (3700) foreshock sequences of $M \geq 4$ mainshocks in the SCEC catalog. The foreshocks have been selected in a time-space window with $T = 200$ days and $R = 30$ km. While we see clearly an acceleration (inverse Omori law $n(t) = (t_c - t)^{-p}$, where t_c is the common stacked mainshock time and $p = 0.9 \pm 0.1$) for the averaged foreshock number (black line), there are huge fluctuations of the rate of foreshocks for individual sequences. Most foreshock sequences are characterized by the occurrence of a major earthquake before the mainshock, which has triggered the mainshock most probably indirectly due to a cascade of multiple triggering. For instance, 66 days before its occurrence, the $M = 7.3$ Landers earthquake (upper curve) was preceded by the $M = 6.1$ Joshua-Tree earthquake. The successive oscillations of the cumulative number of events after the Joshua-Tree earthquake correspond to secondary, tertiary, etc., bursts of triggered seismicity.

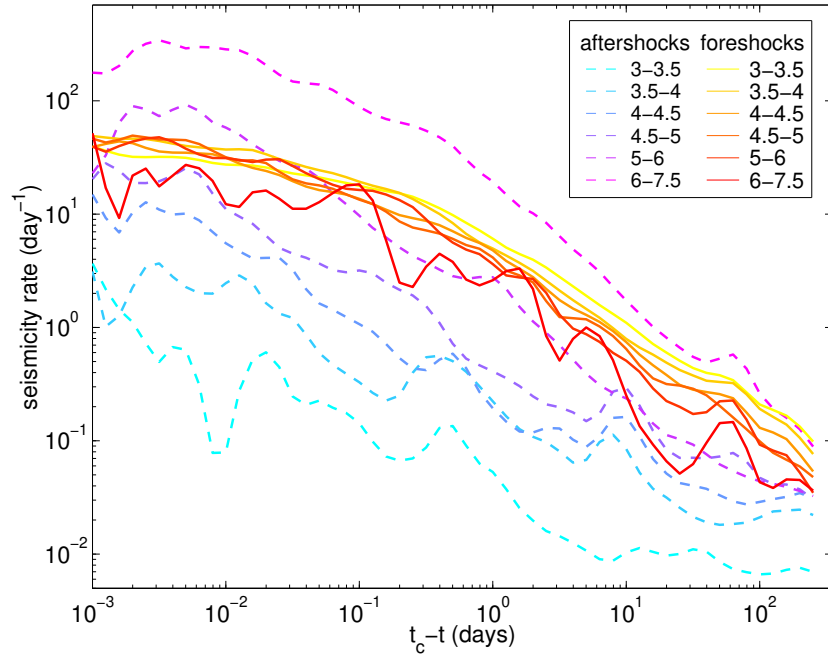


Figure 2: Rate of seismic activity per mainshock for foreshocks of type II (continuous lines) defined in the technical part 6 and for aftershocks (dashed lines) measured as a function of the time $t_c - t$ from the mainshock occurring at t_c , obtained by stacking many earthquake sequences for different mainshock magnitude intervals given in the inset panel. The space-time window used to select foreshocks and aftershocks is ($T = 1$ yr; $R = 50$ km). The fluctuations of the rate of foreshocks are larger for large mainshocks, because the number of mainshocks (resp. foreshocks) decreases from 15584 (resp. 1656249) for the magnitude range $3 \leq M < 3.5$ down to 47 (resp. 1899) for $M > 6$ mainshocks. In contrast, the fluctuation of the rate of aftershocks are larger for small mainshocks magnitudes, due to the increase of the number of aftershocks per mainshock with the mainshock magnitude, and to the rules of mainshock selection which reject a large proportion of small earthquakes. The number of mainshocks is different for aftershocks and foreshocks due to their distinct definition. The number of mainshocks associated with aftershocks decreases from 677 for the magnitude range $3 \leq M < 3.5$ down to 39 for $M \geq 6$ mainshocks. The number of aftershocks increases from 2614 for $3 \leq M < 3.5$ up to 7797 for $M \geq 6$ mainshocks. The truncation of the seismicity rate for small times $t_c - t < 1$ day, especially for aftershocks of large $M \geq 6$ mainshocks and for foreshocks, is due to the incompleteness of the catalog at very short times after mainshocks due to the saturation of the seismic network. At large times from the mainshock, the seismicity rate decreases to the level of the background seismicity, as seen clearly for the rate of aftershocks following small $M = 3$ mainshocks.

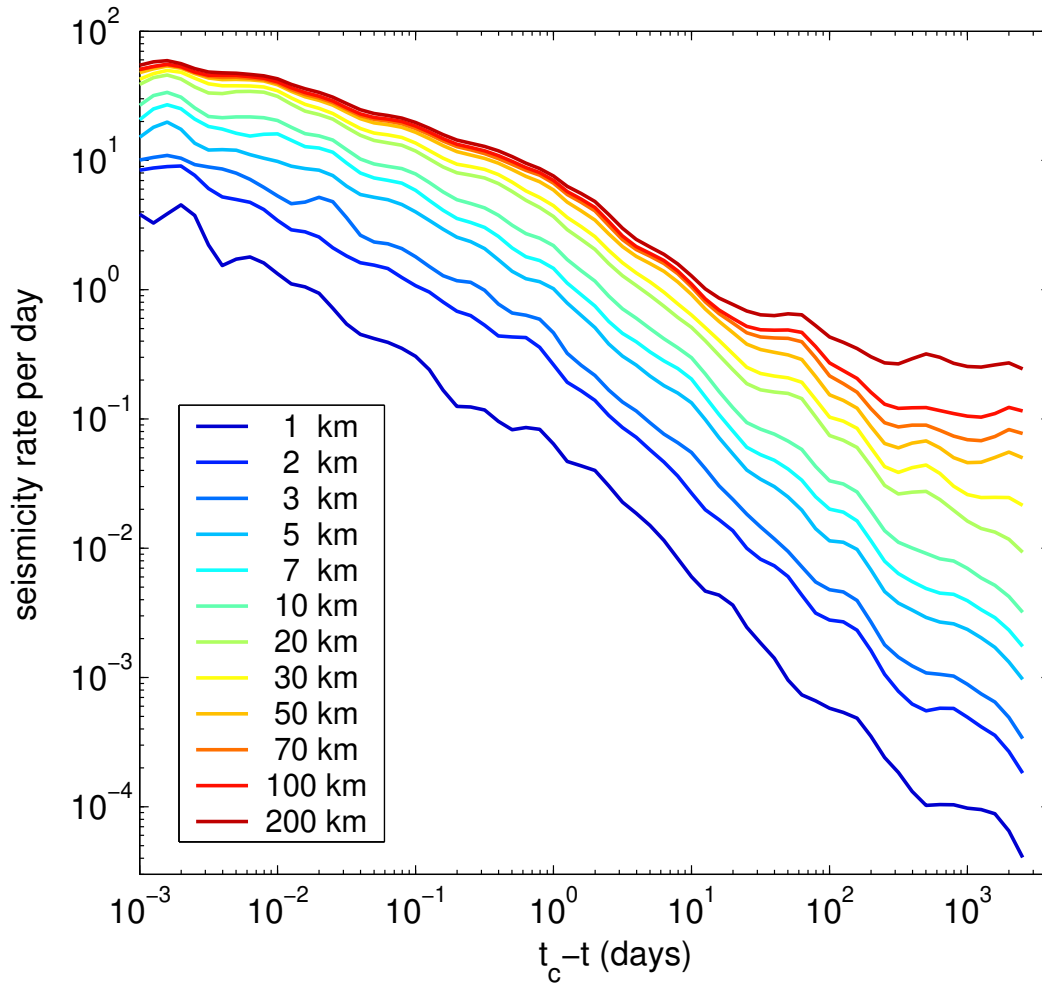


Figure 3: Rate of foreshocks of type II (defined in the technical part 6) averaged over 2158 mainshock with magnitudes in the range (4;4.5), for $T = 10$ yrs and for different choices of the distance R between 1 and 200 km used to select foreshocks around mainshocks. The total number of foreshocks of type II increases from 1001 for $R = 1$ km up to 2280165 for $R = 200$ km.

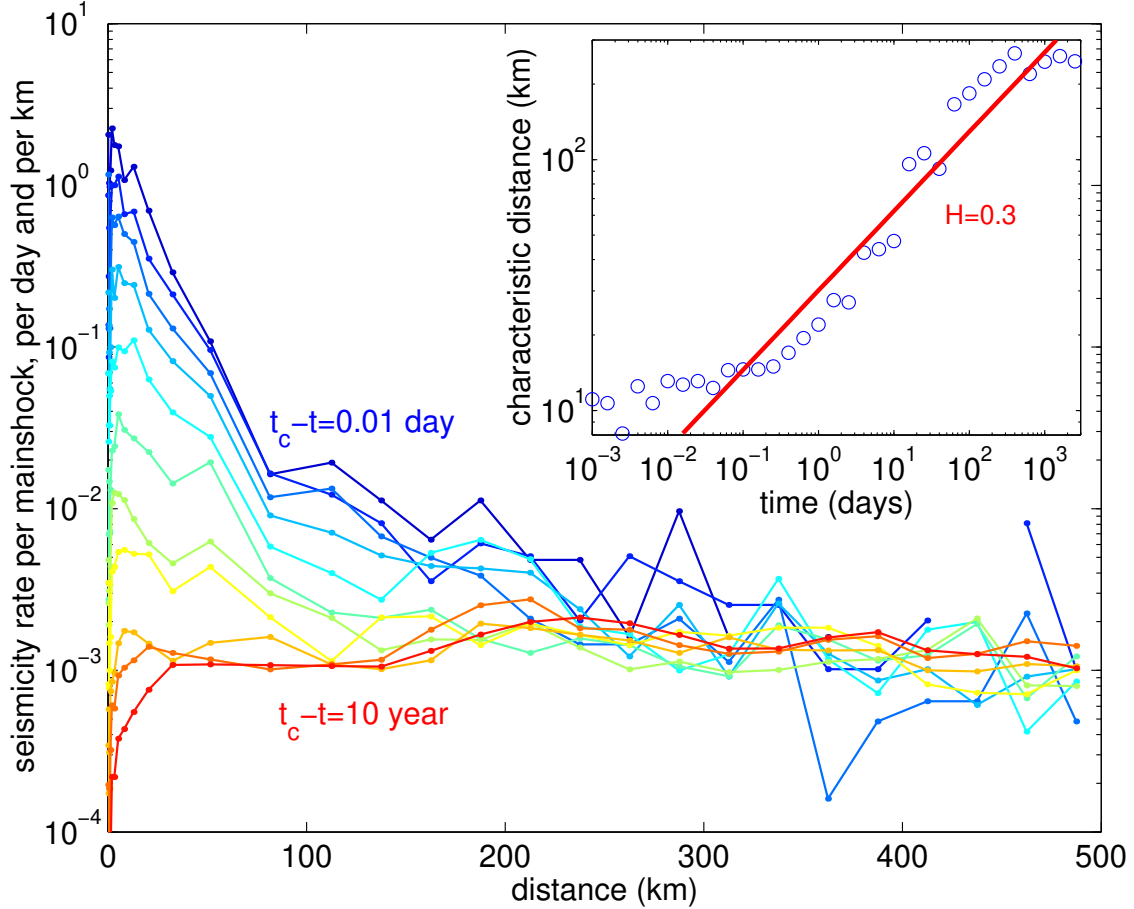


Figure 4: Rate of foreshocks of type II (defined in the technical part 6) before $M = 4.5$ mainshocks as a function of the distance from the mainshock for different values of the time before the mainshock. We use logarithmic bins for the time windows, with a bin size increasing from 0.01 day up to 10 yrs as a geometric series with multiplicative factor 3.2. The number of events in each time window increases from $N = 936$ for 0.01–0.03 days up to 2096633 for 1000–3650 days. We evaluate the seismicity rate for different distances from the mainshock by counting the number of events in each shell $(r; r + \Delta r)$. The seismicity rate is normalized by the number of mainshocks, the duration of the time window and the widths of the space window Δr (controlling the discretization of the curves) used to estimate the seismicity rate. The inset shows the characteristic size of the cluster of foreshocks, measured by the median of the distance between all foreshock-mainshock pairs, as a function of the time before the mainshock. The solid line is a fit by a power-law $R \propto t^H$ with $H = 0.3$. Due to the large space-time window $T = 10$ yrs and $R = 500$ km used to select foreshocks, a large proportion of the seismicity are background events, which induces a spurious migration of seismicity toward the mainshock (see section 4).

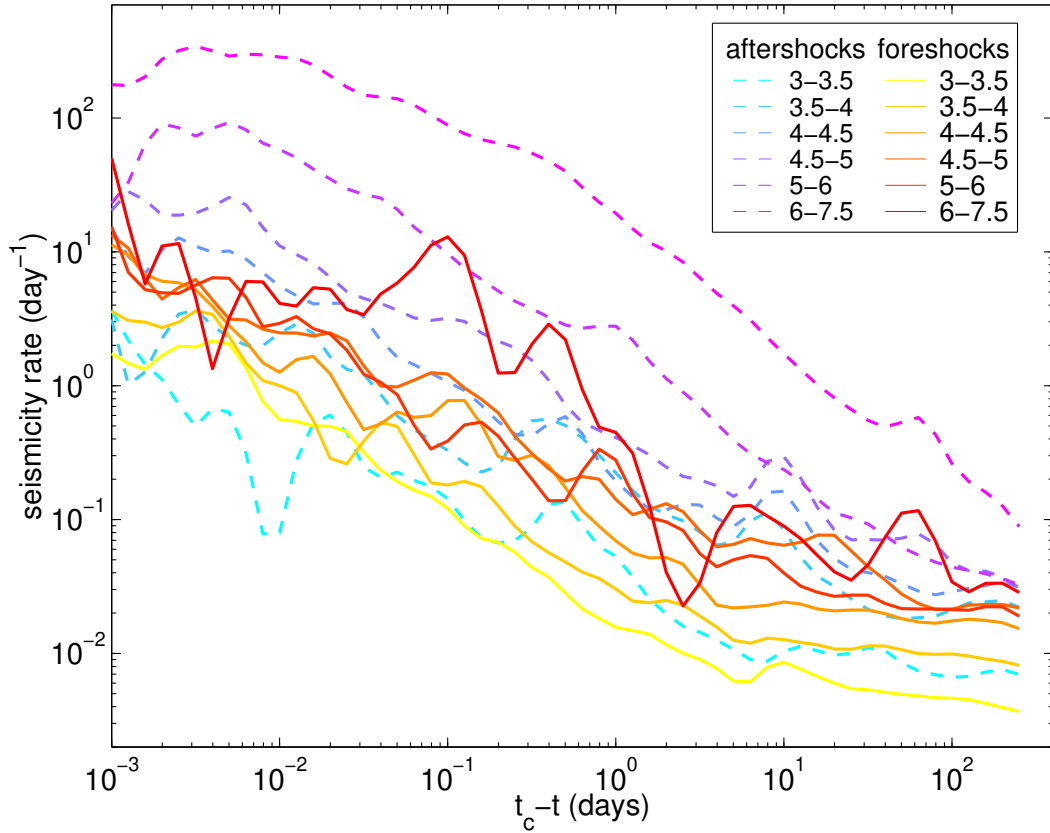


Figure 5: Same as Figure 2 for foreshocks of type I (defined in the technical part 6) which have been selected using a space-time window $R = R_2 = 50$ km and $T = 1$ yr. The presented data and the statistics for aftershocks are the same as in figure 2. The total number of foreshocks of type I is much smaller than the number of type II foreshocks for small mainshocks because a significant fraction of foreshocks of type II are “aftershocks” of large $M > 6$ earthquakes according to the usual definition and are therefore rejected from the analysis of foreshocks of type I, which are constrained to be smaller than their mainshock. The total number of foreshocks of type I ranges from 1050 to 5462 depending on the mainshock magnitude. The same mainshocks are used for the selection of aftershocks and of type I foreshocks.

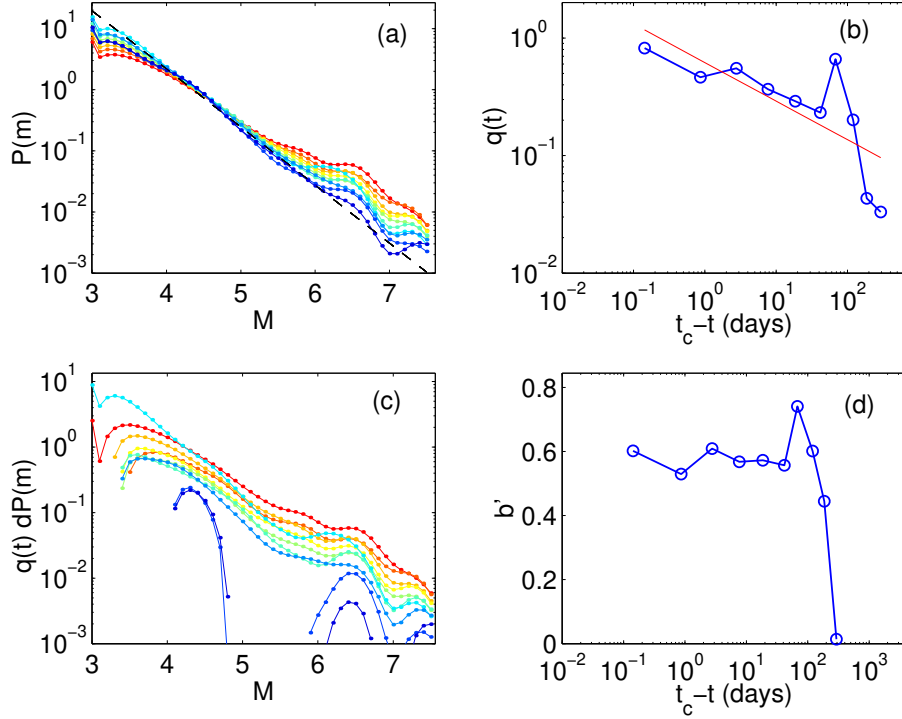


Figure 6: (a) Magnitude distribution $P(m)$ of foreshocks of type II using a space-time window $R = 20$ km and $T = 1$ yr before each earthquake. Note the progressive transition from a concave to a convex shape; (c) deviatoric distribution $q(t)dP(m)$ measured for 10 time windows of equal number of events. The grey scale of each curve in (a) and (c) ranges from blue to red as the time $t_c - t$ from the mainshock decreases from 1 yr to 0.01 day. The truncation for small magnitudes $m < 4$ is due to the incompleteness of the catalog just after large earthquakes. The foreshock magnitude distribution is well fitted in the magnitude range $4 < m < 7$ by the sum of two power-laws (1), with an exponent $b^0 = 0.6$ independently of the time from the mainshock. The exponent b^0 of $dP(m)$ shown in panel (d) is approximately constant for all time periods, except at very long times before the mainshock where it drops to 0 when the amplitude $q(t)$ of the deviatoric distribution becomes too small. The amplitude $q(t)$ of the deviatoric distribution is shown in panel (b) with a power law fit as a function of $t_c - t$ with exponent 0.3 ± 0.2 shown as the straight line. Quantitatively, b^0 is marginally outside the 2 -confidence interval for the prediction $b^0 = b = 0.2 \pm 0.2$ using the estimation $b = 0.8 \pm 0.1$ [39] that allows us to collapse the aftershocks shown in figures 2 and 5 onto a single master curve (not shown here but see Ref. [39]). We attribute this discrepancy to the dual impact of the incompleteness of the catalog for small magnitudes after a large earthquake and to the smallness of the statistics. We stress that the prediction (1) with $b^0 = b$ has been verified with good precision in synthetic catalogs which do not have these limitations [34]. Using the best fitted value $b^0 = 0.6$, we obtain a reasonable agreement for the predicted exponent $b^0 = 0.6$ and the fitted value 0.3 ± 0.2 for the power law behavior of $q(t)$ using $b = 0.8 \pm 0.1$ in the range $0.2 < t_c - t < 0.4$.